Chaos
An Interdisciplinary Journal
of Nonlinear Science

AIP Publishing

Oscillatory dynamics in a reaction network based on imine hydrolysis

Emese Lantos,[1] Ágota Tóth,[1] and Dezső Horváth[2, a)]
[1)] *Department of Physical Chemistry and Materials Science, University of Szeged, Rerrich Béla tér 1., Szeged, H-6720, Hungary*
[2)] *Department of Applied and Environmental Chemistry, University of Szeged, Rerrich Béla tér 1., Szeged, H-6720, Hungary*

(Dated: 16 September 2023)

We have built an autocatalytic reaction network, based on the hydrolysis of certain imines, which exhibits bistability in an open system. The positive feedback originates from the interplay of fast acid-base equilibria, leading to hydroxide ion production, and pH-dependent hydrolysis rates. The addition of a first-order removal of the autocatalyst can result in sustained pH oscillations close to physiological conditions. The unit-amplitude pH oscillations are accompanied by the stoichiometric conversion of imine into amine back and forth. A systematic parameter search is carried out to characterize the rich observable dynamics and identify the evolving bifurcations.

Autocatalysis rarely appears at the level of simple elementary reactions but rather arises from complex reaction networks. Rapid changes of composition, as chemical equilibria shift, can provide sufficiently strong nonlinear concentration dependence that can destabilize steady states in open systems. Bistable switches and oscillations are essential features of biologically important networks, and their existence is driven by intrinsic positive feedback. Acid-base equilibria around physiological pH, for example, are sensitive to small changes in the hydroxide ion concentration, therefore coupling with pH-dependent reaction rates can lead to large nonlinear responses. This can produce a chemical signal that can maintain biochemical control in larger networks. The studied model, based on imine hydrolysis, is an example where the proximity of two acid-base equilibria allows interactions with hydroxide-dependent reaction rates to drive oscillations.

I. INTRODUCTION

Autocatalysis has a long history since its name was defined by Ostwald in 1890[1]. According to the original definition, we regard reactions autocatalytic, if at least one product can catalyze its own formation[1–4]. However, this notion has been extended because we now know that not only a single reaction but also an entire reaction network can exhibit autocatalytic features even if there isn't any autocatalytic step involved. Positive feedback in these systems evolves from the interconnection of reaction steps. Autocatalytic processes can be classified based on various aspects[4,5], such as the strength of autocatalysis, the effectiveness, the mechanism of the process[2,3], or the chemical nature[6–8] whether it is an organic, inorganic, acid or base autocatalysis.

In the last decades, autocatalysis has been one focus of interest in the quest to unravel the difficult questions of the emergence of life[9–13]. The envisioned scenario is out-of-equilibrium conditions with nonlinear responses to external chemical stimuli that can lead to local decrease of entropy allowing the growth of complexity[14]. For that in any chemical systems emergent properties and functions can only evolve via inherent positive feedback within the network of reactions[15,16]. In cellular life many important functions are governed by complex dynamics[17]. Signal transmission may rely on kinetic switches where bistability plays a vital role[18,19].

In enzymatic cycles the pH of the medium is an important parameter because it determines the molecular structure and hence controls selectivity and functioning. The first pH oscillators were based on the use of strong inorganic acids and oxidative compounds that resulted in large pH amplitudes[8,20,21]. Generally, they can be divided into one-substrate and two-substrate classes based on the number of substrates[8,22]. Their mechanism is comparatively simple: it involves the autocatalytic production of hydrogen ion in a redox reaction as a positive feedback and its removal ensuring the negative feedback. By taking advantage of the periodic changes in redox potential or pH, one can drive gelation processes where the accompanying periodic swelling-deswelling can lead to self locomotion[23,24], control aggregation of nanoparticles into supramolecular structures, vesicle-to-micelle transitions[25], or produce highly ordered biomorph structures by regulating antagonistic precipitation processes[26]. Coupling of a pH oscillator with a pH-sensitive hydrogel[27] can introduce chemomechanical instabilities[28] and open possibilities for controlled drug delivery[29].

Organic oscillators, starting with the methylene glycol-sulfite-gluconolactone reaction[30], have opened new possibilities for coupling at milder conditions, where supramolecular assemblies with hydrogen bonds can be driven.[31] They represent an important step towards in-

[a)] E-mail: horvathd@chem.u-szeged.hu

creasing the biocompatibility of chemical oscillators. Realizing pH oscillations around physiological pH alone are not sufficient, the components within the reaction network cannot be toxic to the coupled system[8]. Because the hydrogen ion concentration is small within this range, for constructing robust systems the involvement of protonation-deprotonation equilibria is needed. In addition to pH-dependent enzyme activity[32] or hydrogel swelling[33,34], a fast shift in equilibrium composition can also cause an amplified nonlinear response to provide strong feedback. In our earlier work we have shown that the proximity of two acid-base equilibria in the hydrolyisis of certain imines can result in autocatalysis when hydroxide ion production occurs around physiologial pH.[35]

In this work we explore the autocatalytic reaction network based on the hydrolysis of salicylaldehyde-based imines coupled to slow hydroxide ion removal in an open system. By the systematic variation of parameters, we map the region of bistability and oscillations, characterize the stable steady states and limit cycles. This allows us to identify the driving force of instability in a reaction network where the individual steps are not associated with high kinetic order, a requirement considered necessary in the classical description of chemical autocatalysis.

II. MODEL SYSTEM

During the hydrolysis of an imine, an amine and an aldehyde form. The reaction network consists of several steps according to

$$\mathrm{S} + (\mathrm{H_2O}) \rightleftharpoons \mathrm{SH^+} + \mathrm{OH^-} \qquad \frac{k_1}{k_{-1}} = K_1 \quad (1)$$

$$\mathrm{SH^+} + \mathrm{OH^-} \rightarrow \mathrm{B} + \mathrm{Ox} \qquad k_2 \quad (2)$$

$$\mathrm{B} + (\mathrm{H_2O}) \rightleftharpoons \mathrm{BH^+} + \mathrm{OH^-} \qquad \frac{k_3}{k_{-3}} = K_3 \quad (3)$$

$$(\mathrm{H_2O}) \rightleftharpoons \mathrm{H^+} + \mathrm{OH^-} \qquad \frac{k_4}{k_{-4}} = K_4 \quad (4)$$

$$\mathrm{SH^+} + (\mathrm{H_2O}) \rightarrow \mathrm{BH^+} + \mathrm{Ox} \qquad k_5 \quad (5)$$

$$\mathrm{S} + \mathrm{OH^-} \rightarrow \mathrm{Ox^-} + \mathrm{B} \qquad k_6 \quad (6)$$

$$\mathrm{Ox^-} + (\mathrm{H_2O}) \rightleftharpoons \mathrm{Ox} + \mathrm{OH^-} \qquad \frac{k_7}{k_{-7}} = K_7 \quad (7)$$

where the parentheses indicates that the concentration of the solvent water is considered constant due to its large excess.[35] Reactions (1)-(5) comprise the general imine hydrolysis: the protonation of the imine (S) and the amine (B) in Eqs. (1) and (3), respectively; the OH-dependent and direct reactions of the protonated imine (SH^+) in Eqs. (2) and (5); the autoprotolysis of water in Eq. (4). In addition, for imines originating from salicylaldehyde, the reaction between imine and hydroxide ion in Eq. (6) takes place followed by the protonation of the deprotonated salicylaldehyde (Ox^-) in Eq. (7). In this model, the acid-base reactions in Eqs. (1), (3), (4), and (7) are considered as reversible reactions. The conversions of imine into amine and aldehyde in Eqs. (2), (5), and (6) are taken as irreversible steps because the reactant concentration is low in the experiments,[35] upon the results of which this model is based.

In this reaction network there is no single step that would be autocatalytic, the interconnection of the individual reactions yields the positive feedback associated with the entire network. Amines are generally stronger bases than imines, resulting in $K_3 > K_1$, hence the concentration of hydroxide ion increases during the hydrolyses of imines.[35] By inspecting the three parallel pathways for the conversion of imine into amine, we can see that the one in Eq. (5) is independent of hydroxide ion, while both in Eqs. (2) and (6) have rates increasing with hydroxide ion concentration. The latter is found to be crucial because it forms a catalytic pathway with Eq. (7) as

$$\mathrm{S} + \mathrm{OH^-} \rightarrow \mathrm{B} + \mathrm{Ox} + \mathrm{OH^-} \quad (8)$$

since the equilibrium in Eq. (7) is shifted to the right.

This network itself can exhibit bistability under conditions corresponding to a continuously-stirred tank reactor.[35] Here we explore its capabilities with the addition of a general first-order removal of hydroxide ion as

$$\mathrm{OH^-} \rightarrow \mathrm{P} \qquad k_r \quad (9)$$

where P stands for an inert product species.

The governing equations are now in the form of

$$\frac{dc_i}{dt} = \sum_{j=1}^{12} \nu_{i,j} r_j + k_0 \left(c_{i,0} - c_i\right) \quad (10)$$

where c_i is the concentration of the species (S, SH^+, B, BH^+, H^+, OH^-, Ox^-, Ox) with stoichiometric coefficients $\nu_{i,j}$ in the 12 reactions of Eqs. (1)–(7) and (9) with rates r_j. The inverse of residence time is the flow rate k_0 and $c_{i,0}$ is the concentration in the input feed which contains only the imine at a set pH.

The numerical analysis of the 8-variable model was carried by using the `XPPAUT` software package. For the temporal evolution of concentrations the initial value problem in Eq. (10) was solved by the `CVODE` solver integrated within `XPPAUT`. From the stable steady states, obtained by the direct integration, the bifurcation analysis was performed by `AUTO`, also built-in `XPPAUT`. During the stability analysis of the steady states, the bifurcation points were continued in a two-dimensional parameter space to map the regions of bistability or oscillations. From the Hopf-bifurcations the oscillatory solutions were also continued with `AUTO` to monitor the period of oscillations.

The parameter set summarized in Table I is related to the experimental system of our earlier study.[35] The equilibria in Eqs. (1), (3), (4), and (7) basically occur on a faster time scale with diffusion-limited reverse steps

($k_{-1} = k_{-3} = k_{-4} = k_{-7} = 5 \times 10^8$ $M^{-1}s^{-1}$). The ordinary differential equations were solved with the BDF routine and the relative tolerance was set to 10^{-8}. For the bifurcation mapping the typical minimum (DSMIN) was 10^{-8} with epsilon (EPSS) of 10^{-10}.

TABLE I. The parameter set used in the numerical study

Parameters	Values and units
K_1	8×10^{-11} – 8×10^{-8} M
K_3	2.7×10^{-5} – 2.7×10^{-2} M
K_4	1×10^{-14} M
K_7	7×10^{-7} – 1×10^{-3} M
k_2	1.2×10^{4} $M^{-1}s^{-1}$
k_5	0 – 0.020 s^{-1}
k_6	1.2×10^{3} $M^{-1}s^{-1}$
k_0	0 – 0.1 s^{-1}

III. RESULTS AND DISCUSSIONS

A. Steady states

First, we looked at the contribution of the direct hydrolytic step in Eq. (5), the rate of which is independent of hydroxide ion concentration. In the absence of removal, i.e., $k_r = 0$ s^{-1}, the steady state at low flow rate is characterized with high conversion, yielding higher hydroxide ion concentration (see Fig. 1). With decreasing residence time, i.e., increasing k_0, the concentrations approach that of the input feed. There is a single stable steady state in the entire regime with significant contribution of the direct hydrolysis. The bistability window appears only upon decreasing the value of k_5 that enhances the positive feedback associated with the catalytic step in Eq. (6).

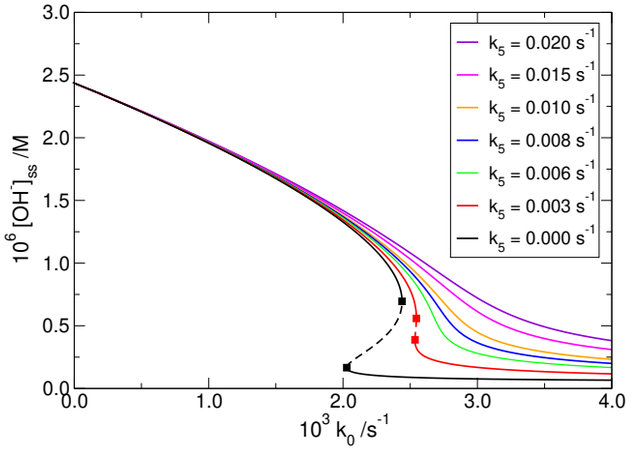

FIG. 1. Steady state concentrations of hydroxide ion as a function of flow rate k_0 for systems with different contributions of the direct step in the absence of OH^--removal with $K_1 = 8\times10^{-9}$ M, $K_3 = 2.7\times10^{-5}$ M, and $K_7 = 7\times10^{-7}$ M. The solid lines represent stable steady states, while the dashed lines connect the unstable ones.

We then introduce the removal of hydroxide ion with a first-order reaction and vary its contribution by changing the rate coefficient k_r. The removal has the largest effect on the thermodynamic branch at longer residence time, where it decreases the steady state hydroxide concentration as shown in Fig. 2(a,b). The direct step, on the other hand, has larger effect at smaller residence time where k_0 is greater: the folding of steady states allowing multiple solutions gradually vanishes as k_5 is increased (see Fig. 2(c,d)), similarly to the case in the absence of hydroxide removal.

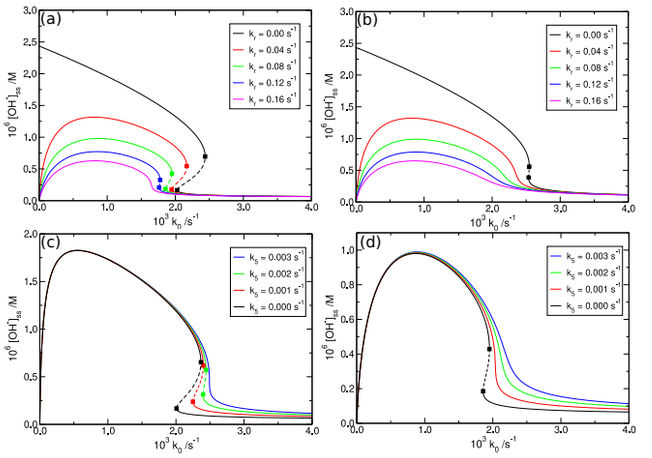

FIG. 2. Steady state concentrations of hydroxide ion as a function of flow rate k_0 with changing contribution of the direct step (k_5) or the removal step (k_r) with (a) $k_5 = 0$ s^{-1}, (b) $k_5 = 0.003$ s^{-1}, (c) $k_r = 0.01$ s^{-1}, and (d) $k_r = 0.08$ s^{-1}. In all cases $K_1 = 8\times10^{-9}$ M, $K_3 = 2.7\times10^{-5}$ M, and $K_7 = 7\times10^{-7}$ M. The solid lines represent stable steady states, the dashed lines connect the unstable ones, and the symbols denote the saddle-node bifurcations.

By following the saddle-node bifurcation in a 2-dimensional parameter space, we map out the region of multiple steady states in Fig. 3. The figure reveals that the direct hydrolysis not only diminishes this region but also shifts it to smaller residence time, i.e., to greater k_0 flow rates.

B. Hopf bifurcation

The removal of hydroxide ion also decouples the temporal time scale associated with OH^- from that of the rest. This allows the destabilization of the thermodynamic branch via Hopf bifurcation. Considering the bistable scenario with $k_5 = 0$ s^{-1}, as k_r increases a subcritical Hopf bifurcation point evolves out of the saddle-node bifurcation at the end of the thermodynamic branch. The unstable limit cycle around the stable steady state vanishes in a saddle-loop bifurcation as

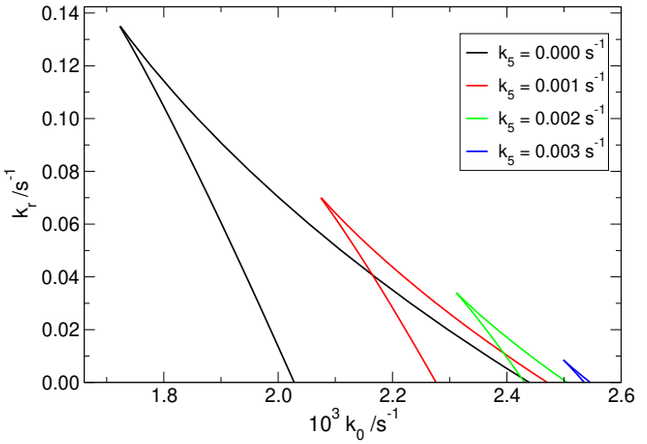

FIG. 3. Saddle-node bifurcation points bounding the region of multiple steady states with parameters given in Fig. 2.

shown in Fig. 4(a) for larger values of K_1 and K_7. The region of bistability hence shrinks within the zone of multiple steady states, it is now limited between the saddle-node bifurcation (at lower k_0) and the Hopf bifurcation. Upon increasing k_r, both the Hopf and the saddle-loop bifurcation points shifts to the left, further decreasing the region of bistability. At the lower limit point, a stable limit cycle appears as a double-loop bifurcation evolves out of the saddle-loop (see Fig. 4(b-c)). This shifts left to lower k_0 into the monostable region and later collides with the Hopf bifurcation, turning it into a supercritical type, as presented in Fig. 4(d). Figure 5 depicts the

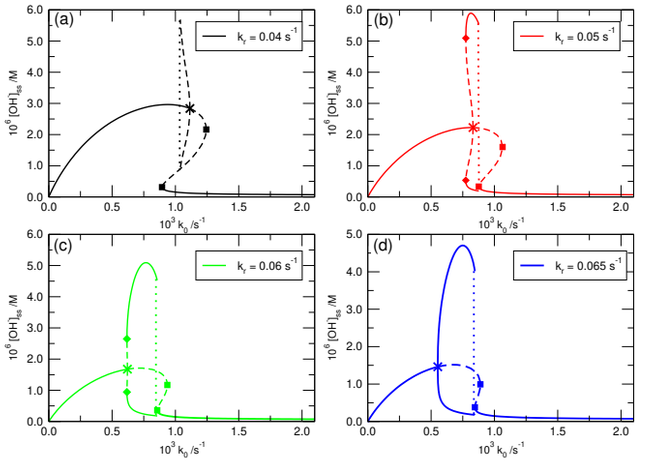

FIG. 4. Steady state concentrations of hydroxide ion as a function of flow rate k_0 at different k_r values of (a) $k_r = 0.04\ \mathrm{s}^{-1}$, (b) $k_r = 0.05\ \mathrm{s}^{-1}$, (c) $k_r = 0.06\ \mathrm{s}^{-1}$, and (d) $k_r = 0.065\ \mathrm{s}^{-1}$. In all cases $K_1 = 8 \times 10^{-8}$ M, $K_3 = 2.7 \times 10^{-5}$ M, $K_7 = 1 \times 10^{-3}$ M, and $k_5 = 0\ \mathrm{s}^{-1}$. The solid lines represent stable steady states, the dashed lines connect the unstable ones, and the saddle node bifurcations are indicated by dotted lines with the symbols denoting the other bifurcations.

relative location of the range of stable oscillations and bistability that comprises a cross-shaped diagram[36] in the k_r–k_0 parameter plane.

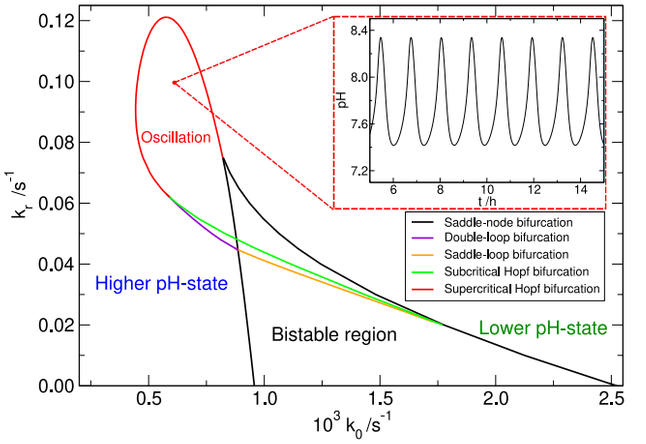

FIG. 5. Phase diagram of the reaction network in the absence of direct hydrolysis with parameters given in Fig. 4. Inset shows the pH trace at a point within the range of oscillations.

The dynamics around the steady states is governed by the two largest eigenvalues obtained by the linear stability analysis, the rest remain negative in the entire parameter range. As we follow the steady state from the flow branch (large k_0) to the thermodynamic branch (low k_0), we cross the $(\lambda_1 + \lambda_2)$-axis twice representing the saddle-node bifurcations and once the $(\lambda_1\lambda_2)$-axis revealing a Hopf bifurcation, as shown in Fig. 6 in an analogy to the trace–determinant presentation of two-variable systems.

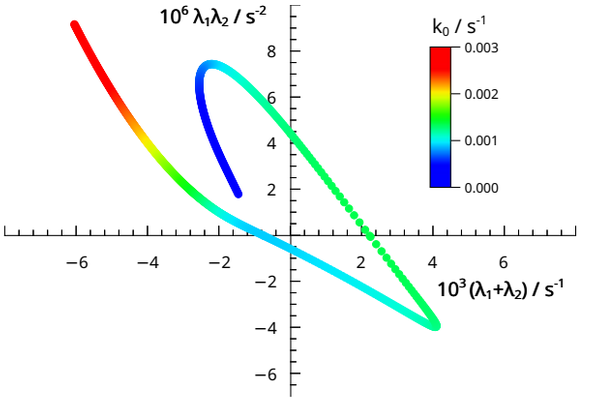

FIG. 6. Variation of the two largest eigenvalues along the steady state from the flow branch to the thermodynamic branch. Saddle-node bifurcations occur on crossing the $(\lambda_1 + \lambda_2)$-axis, Hopf bifurcation is located at the intersection with the $(\lambda_1\lambda_2)$-axis with parameters given in Fig. 4 and $k_r = 0.04\ \mathrm{s}^{-1}$.

On the one hand, the reverse step in Eq. (7) only plays a role at higher pH, therefore an increase in the value of K_7 does not cause a significant change in the phase

diagram of Fig. 5. On the other hand, the interplay between K_1 and K_3 is essential for the existence of the rich dynamics. Larger separation of the two equilibrium constants simplifies the observable phenomenon. As K_1 is decreased (see Fig. 7), the region of oscillation vanishes. The increase of K_3 at the same time shrinks the region of

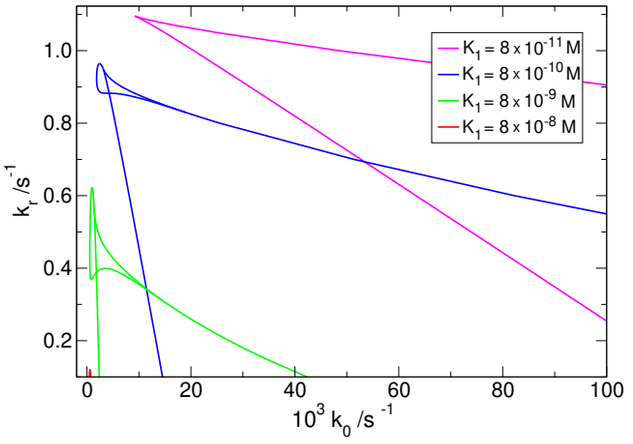

FIG. 7. Phase diagram of the reaction network on decreasing K_1 while using the other parameters given in Fig. 4.

bistability as shown in Fig. 8. It is important to point out

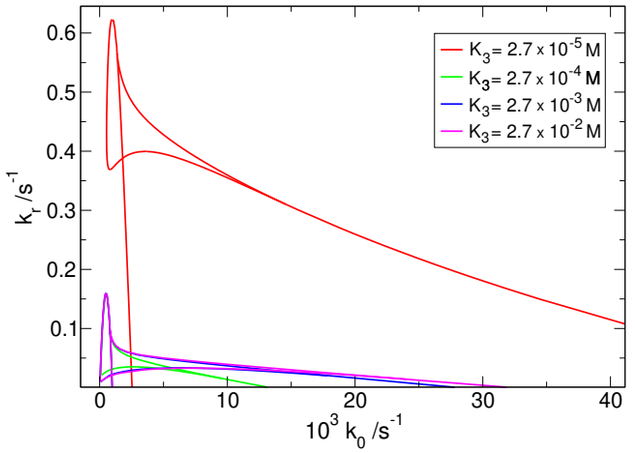

FIG. 8. Phase diagram of the reaction network on increasing K_3, while using the other parameters given in Fig. 4.

that while the pH difference between the flow and thermodynamic branches is small, the switch between them is accompanied by a stoichiometric conversion of imine into amine (from 30 % to 90 %) or back (see Fig. 9). In this pH range the weaker base imine remains dominantly deprotonated, i.e., $[S] > [SH^+]$, while the stronger base amine is mainly in its protonated form as $[BH^+] > [B]$ (see Fig. 9(a-b)). This maintains the scenario at which hydroxide ion is produced during the imine hydrolysis, which drives the positive feedback in the network. The interplay of the two acid-base equilibria ensures that the conversion of imine to amine does not require large pH change, thus keeps the solution close to neutral.

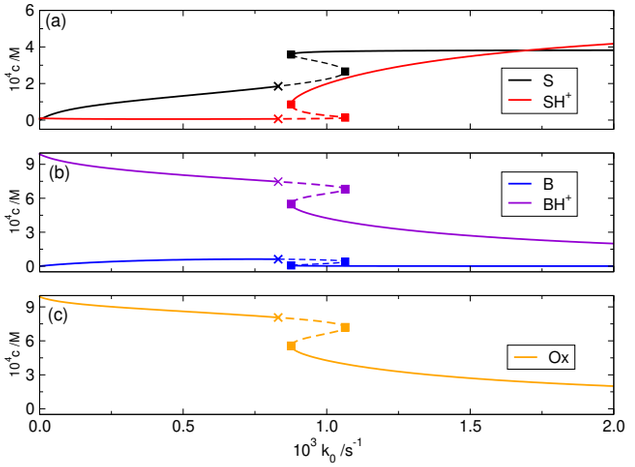

FIG. 9. The concentration of key species under conditions corresponding to Fig. 4(b).

C. Oscillatory dynamics

The characteristics of temporal oscillations are mapped by continuing the limit cycle solutions that emerge from the Hopf bifurcations. For an example scenario, we present stable oscillations sandwiched between a double-loop and a saddle-loop bifurcation in Fig. 10. While the amplitude of the pH oscillations varies little in the entire range with ΔpH=1.0–1.4 on increasing k_0, the period of stable oscillations increases exponentially upon approaching the homoclinic orbit ($k_0 > 8.7 \times 10^{-4}$ s^{-1}), as shown in Fig. 10(b).

Even though the amplitude of pH oscillation is greater than the pH difference between the flow and thermodynamic branches, it is still considered small. Yet, within an oscillatory cycle a stoichiometric conversion of imine into amine (from 50 % to 80 %) and back takes place. The sharp increase in the hydroxide ion concentration is accompanied by a fast conversion of imine into amine and the latter quickly becomes protonated because it is a stronger base. The removal of OH^- then diminishes the concentration of OH^- on the same time scale, while the inflow of the fresh reactant only slowly replenishes the imine-amine ratio to that observed in the flow branch. With the increase of k_0 this slow return lengthens along with the period, the width of OH^- peak remains approximately invariant (see Fig. 10(c)). This is because the limit cycle in the phase space approaches the saddle close to the flow branch. Overall, the period of oscillation mainly depends on the distance from the saddle-loop bifurcation, which can also be varied by changing for example, K_1, k_r, or k_5 (see Supplementary Material).

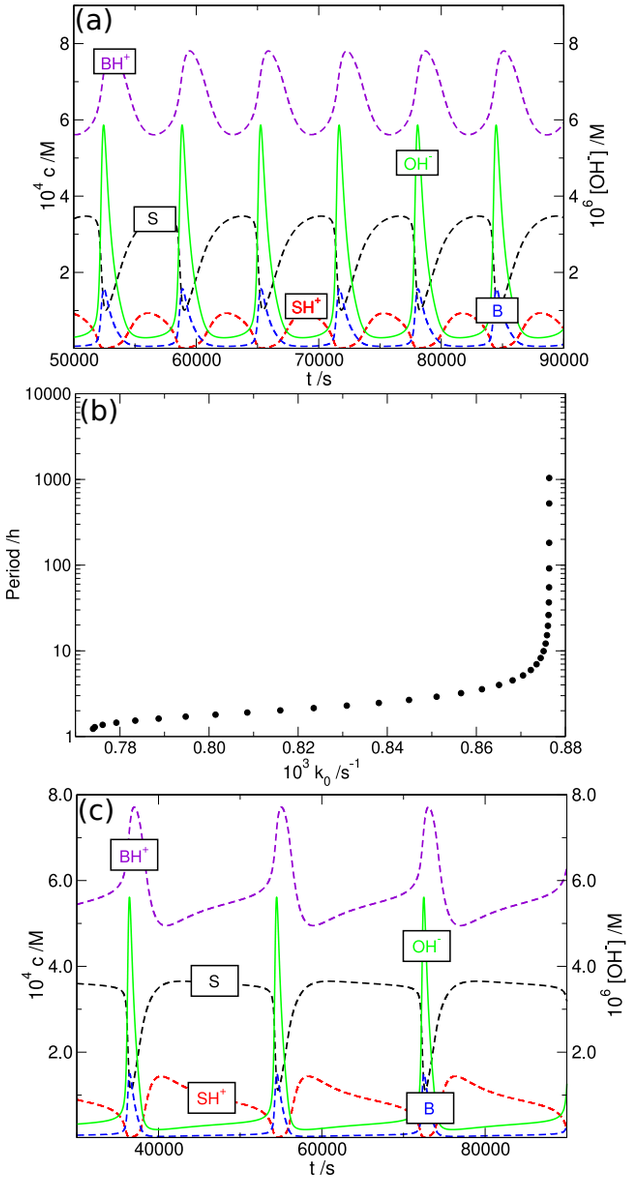

FIG. 10. Concentrations within the stable oscillatory cycles at $k_0 = 8.0{\times}10^{-4}$ s^{-1} (a) and at $k_0 = 8.7{\times}10^{-4}$ s^{-1} (c), along with the change in the period of oscillations as k_0 is increased (b) with $k_r = 0.05$ s^{-1} and using the other parameters given in Fig. 4.

IV. CONCLUSIONS

Numerical simulations and systematic parameter variations are exploited to map out the rich dynamics in an autocatalytic network based on the hydrolysis of an imine. The key element in the network is the interaction of acid-base equilibria with reactions having [OH$^-$]-dependent rates. Although both imines and amines are weak bases, in the appropriate pair the latter is somewhat stronger. This yields a narrow pH-range close to neutral conditions, where the hydrolysis of the imine into amine is accompanied by the production of hydroxide ion. In the base case corresponding to the experimental system[35], there are three parallel pathways that convert the imine into amine and salicylaldehyde: one with rate independent of pH, one that consumes hydroxide ion, and one that is catalytic with respect to hydroxide ion. The interplay of the latter with the hydroxide production from acid-base equilibria is the main driving force that leads to the appearance of bistability. The flow and thermodynamic branches overlap in a pH-range close to the neutral solution. Although the pH gap between the two stable states is small, their composition is significantly different. This allows switches with stoichiometric composition change between the two states from small pH perturbations.

The introduction of a slow hydroxide ion removal reaction can lead to oscillatory behavior in the vicinity of the bistable region. The limit cycle emerges from a Hopf bifurcation on the thermodynamic branch at larger residence time, and vanishes at a saddle-loop bifurcation at the end of the flow branch. As the period lengthens on approaching the homoclinic orbit, the low-pH phase within an oscillatory cycle expands, while the spikes in the hydroxide ion concentration exhibit negligible change in their duration. Similarly to the bistable scenario, stoichiometric composition changes accompany the small amplitude pH oscillations in the entire explored range. This is the result of the interplay between the acid-base equilibria. The vicinity of base-ionization constants for the corresponding imine and amine keeps the system close to neutrality, leading to an increase in the strength of the positive feedback within the network. By comparison, in the extreme case of very weak base imine ([S] $\gg$ [SH$^+$]) and very strong base amine ([B] $\ll$ [BH$^+$]) the reaction network shrinks down to a quadratic autocatalysis, leaving only reactions in Eqs. (3) and (8) where the feedback is not sufficiently strong to allow bistability or with Eq. (9) oscillations in an open system. In that scenario a kinetically more complex autocatalyst removal can lead to oscillatory dynamics.[37] Our case study shows that higher apparent autocatalytic order can arise when a fast chemical equilibrium is shifted from one side to the other because the transition itself can take place in a narrow concentration range. This can then couple to the production of the activator, which is an important scenario in biologically relevant system, where high classical kinetic orders are not common, yet fast nonlinear responses are abound. Therefore, large composition changes driven by small variation in the activator concentration can develop. This type of amplification can be energetically effective, since the activator production or consumption does not require excess chemical fuel. In our example, the network is based on the hydrolysis of certain imines, but similar scenarios can be envisioned in pH-regulated systems close to neutral conditions. Nonlinear responses in pH via bistable switches or oscillations can activate and deactivate enzymes by changing their conformation which can be translated into the larger scale production

of chemicals.

V. SUPPLEMENTARY MATERIAL

Additional figures are presented to show the dependence of the period of oscillation on parameters K_1, k_r, or k_5.

ACKNOWLEDGMENTS

This work was financially supported by the National Research, Development and Innovation Office (K138844).

VI. CONFLICT OF INTEREST

The authors have no conflicts to disclose.

VII. DATA AVAILABILITY

The data that support the findings of this study are available from the corresponding author upon reasonable request.

[1]W. Ostwald, "Über autokatalyse," Ber. Verh. Kgl. Sächs. Ges. Wiss. Leipzig, Math.-Phys. Classe **42**, 189–191 (1890).
[2]R. Plasson, A. Brandenburg, L. Jullien, and H. Bersini, "Autocatalyses," J. Phys. Chem. A. **115**, 8073–8085 (2011).
[3]A. J. Bissette and S. P. Fletcher, "Mechanisms of autocatalysis," Angew. Chem. Int. Ed. **52**, 12800–12826 (2013).
[4]A. I. Hanopolskyi, V. A. Smaliak, A. I. Novichkov, and S. N. Semenov, "Autocatalysis: Kinetics, mechanisms and design," ChemSystemsChem. **3**, 1–30 (2021).
[5]A. K. Horvath, "Correct classification and identification of autocatalysis," Phys. Chem. Chem. Phys. **23**, 7178–7189 (2021).
[6]J. Harrison and K. Showalter, "Propagating acidity fronts in the iodate-arsenous acid reaction," J. Phys. Chem. **90**, 225—226 (1986).
[7]K. Kovacs, R. E. McIlwaine, S. K. Scott, and A. F. Taylor, "An organic-based ph oscillator," J. Phys. Chem. A **111**, 549–551 (2007).
[8]M. Orban, K. Kurin-Csorgei, and I. Epstein, "ph-regulated chemical oscillators," Acc. Chem. Res. **23**, 593–601 (2015).
[9]A. Pross, "Stability in chemistry and biology: Life as a kinetic state of matter," Pure Appl. Chem. **77**, 1905–1911 (2005).
[10]A. Pross, "Seeking the chemical roots of darwinism: bridging between chemistry and biology," Chemistry **15**, 8374–8381 (2009).
[11]D. G. Blackmond, "An examination of the role of autocatalytic cycles in the chemistry of proposed primordial reactions," Angew. Chem. Int. Ed. **48**, 386–390 (2009).
[12]D. G. Blackmond, "Autocatalytic models for the origin of biological homochirality," Chem. Rev. **120**, 4831–4847 (2020).
[13]K. Ruiz-Mirazo, C. Briones, and A. De La Escosura, "Prebiotic systems chemistry: New perspectives for the origins of life," Chem. Rev. **114**, 285–366 (2014).
[14]B. J. Cafferty, A. S. Y. Wong, S. N. Semenov, L. Belding, S. Gmür, W. T. S. Huck, and G. M. Whitesides, "Robustness, entrainment, and hybridization in dissipative molecular networks, and the origin of life," J. Amer. Chem. Soc. **141**, 8289–8295 (2019).
[15]S. N. Semenov, L. J. Kraft, A. Ainla, M. Zhao, M. Baghbanzadeh, V. E. Campbell, K. Kang, J. M. Fox, and G. M. Whitesides, "Autocatalytic, bistable, oscillatory networks of biologically relevant organic reactions," Nature **537**, 656–660 (2016).
[16]A. I. Novichkov, A. I. Hanopolskyi, X. Miao, L. J. W. Shimon, Y. Diskin-Posner, and S. N. Semenov, "Autocatalytic and oscillatory reaction networks that form guanidines and products of their cyclization," Nat. Commun. **12**, 2994 (2021).
[17]Z. Dadon, N. Wagner, and G. Ashkenasy, "The road to non-enzymatic molecular networks," Angew. Chem. Int. Ed. **47**, 6128–6136 (2008).
[18]T. J. Bánsági and A. F. Taylor, "Ester hydrolysis: Conditions for acid autocatalysis and a kinetic switch," Tetrahedron **73**, 5018–5022 (2017).
[19]I. Maity, N. Wagner, R. Mukherjee, D. Dev, E. Peacock-Lopez, R. Cohen-Luria, and G. Ashkenasy, "A chemically fueled non-enzymatic bistable network," Nat. Commun. **10**, 4636 (2019).
[20]G. Rabai, M. Orban, and I. R. Epstein, "Systematic design of chemical oscillators. 64. design of ph-regulated oscillators," Acc. Chem. Res. **23**, 258–263 (1990).
[21]R. McIlwaine, K. Kovacs, S. K. Scott, and A. F. Taylor, "A novel route to ph oscillators," Chem. Phys. Lett. **417**, 39–42 (2006).
[22]I. Szalai, K. Kurin-Csörgei, and M. Orbán, "Modelling ph oscillators in open, semi-batch and batchreactors," React. Kinet. Mech. Catal. **106**, 257–266 (2012).
[23]R. Yoshida, T. Takahashi, T. Yamaguchi, and H. Ichijo, "Self-oscillating gel," J. Amer. Chem. Soc. **118**, 5134–5135 (1996).
[24]R. Yoshida and T. Ueki, "Evolution of self-oscillating polymer gels as autonomous polymer systems," NPG Asia Mater. **6**, e107 (2014).
[25]I. Lagzi, D. Wang, B. Kowaltzky, and B. A. Grzybowski, "Vesicle-to-micelle oscillations and spatial patterns," Langmuir **26**, 13770–13772 (2010).
[26]M. Montalti, G. Zhang, D. Genovese, J. Morales, M. Kellermeier, and J. M. Garcia-Ruiz, "Local ph oscillations witness autocatalytic self-organization of biomorphic nanostructures," Nat. Commun. **8**, 14427 (2017).
[27]B. Dúzs, I. Lagzi, and I. Szalai, "Functional rhythmic chemical systems governed by ph-driven kinetic feedback," ChemSystemsChem **5**, e202200032 (2023).
[28]C. J. Crook, A. Smith, R. A. L. Jones, and A. J. Ryan, "Chemically induced oscillations in a ph-responsive hydrogel," Phys. Chem. Chem. Phys. **40**, 1367–1369 (2002).
[29]S. A. Giannos and S. M. Dinh, "Novel timing systems for transdermal drug delivery," Polym. News **21**, 118–124 (1996).
[30]K. Kovacs, R. E. McIlwaine, S. K. Scott, and A. F. Taylor, "ph oscillations and bistability in the methylene glycol–sulfite–gluconolactone reaction," Phys. Chem. Chem. Phys. **417**, 3711–3716 (2007).
[31]J. Leira-Iglesias, A. Tassoni, T. Adachi, M. Stich, and T. M. Hermans, "Oscillations, travelling fronts and patterns in a supramolecular system," Nat. Nanotechnol. **13**, 1021–1027 (2018).
[32]L. F. Olsen, "Complex dynamics in an unexplored simple model of the peroxidase-oxidase reaction," Chaos **33**, 023102 (2023).
[33]X. Fan and A. Walther, "ph feedback lifecycles programmed by enzymatic logic gates using common foods as fuels," Angew. Chem. Int. Ed. **60**, 11398–11405 (2021).
[34]C. Sharma, I. Maity, and A. Walther, "ph-feedback systems to program autonomous self-assembly and material lifecycles," Chem. Commun. **59**, 1125–1144 (2023).
[35]E. Lantos, G. Mótyán, E. Frank, R. Eelkema, J. van Esch, D. Horváth, and A. Tóth, "Dynamics of hydroxide-ion-driven reversible autocatalytic networks," RSC Adv. **13**, 20243–20247 (2023).
[36]J. Boissonade and P. De Kepper, "Transitions from bistability to limit cycle oscillations. theoretical analysis and experimental evidence in an open chemical system," J. Phys. Chem. **84**, 501–506 (1980).

[37]J. Merkin, D. J. Needham, and S. K. Scott, "A simple model for sustained oscillations in isothermal branched-chain or autocatalytic reactions in a well stirred open system i. stationary states and local stabilities," Proc. Roy. Soc. London A **398**, 81–100 (1985).